Translational Oncology
www.transonc.com
Volume 4 Number 4 August 2011 pp. 234–240 234

Immunohistochemical Detection of the CXCR4 Expression in Tumor Tissue Using the Fluorescent Peptide Antagonist Ac-TZ14011–FITC[1,2]

Nynke S. van den Berg*,[3], Tessa Buckle*,[3], Joeri Kuil*, Jelle Wesseling[†] and Fijs W.B. van Leeuwen*

*Departments of Radiology and Nuclear Medicine, The Netherlands Cancer Institute – Antoni van Leeuwenhoek Hospital, Amsterdam, The Netherlands; [†]Department of Pathology, The Netherlands Cancer Institute – Antoni van Leeuwenhoek Hospital, Amsterdam, The Netherlands

Abstract

Pathology is fundamental in grading, staging, and treatment planning of malignancies. One relatively novel biomarker that may become more important in therapy and diagnostics is the chemokine receptor 4 (CXCR4). Ac-TZ14011 peptide derivatives, functionalized with a radiolabel, can be used for molecular imaging of tumors. Direct fluorescent labeling of the small peptide Ac-TZ14011 with the fluorescent dye fluorescein isothiocyanate (FITC), however, provides an alternative for the detection of CXCR4 expression levels in cells and tumor tissue. In this study, Ac-TZ14011–FITC was validated for CXCR4 staining in human breast cancer cell lines MDAMB231 and MDAMB231^{CXCR4+} during flow cytometric analysis. Its efficacy was compared to commercially available antibodies. Competition experiments validated the staining specificity. Confocal imaging revealed that CXCR4 staining was predominantly found on the cell membrane and/or in vesicles formed after endocytosis. Next to being able to differentiate "high" and "low" CXCR4-expressing tumor cells, the fluorescent peptide demonstrates potential in fluorescent immunohistochemistry of tumor tissue. Ac-TZ14011–FITC was able to differentiate MDAMB231 from MDAMB231^{CXCR4+} tumor cells and tissue, proving its applicability in the detection of differences in CXCR4 expression levels.

Translational Oncology (2011) 4, 234–240

Introduction

The chemokine receptor 4 (CXCR4) was first detected as coreceptor for CD4$^+$ T-cell infection in human immunodeficiency virus type 1 [1,2]. More recently, a role for CXCR4 has been described in the attraction of inflammatory cells [3] and the pathogenesis of rheumatoid arthritis [4–6]. Besides its expression in normal tissues, a 5.5-fold up-regulation of CXCR4 expression was found in breast cancer tissue [7], and increased CXCR4 expression levels have been reported for at least 22 other types of cancer [8,9].

The cell membrane–based interaction between CXCR4 and its natural ligand, SDF-1 (stromal cell–derived factor 1; CXCL12), is considered to be a driving factor [3] in its role as cellular chemoattractant [10]. CXCR4-based chemoattraction acts directly on tumor cell migration and invasion toward an SDF-1 gradient [11]. High expression levels of SDF-1 have been found at the most common sites of breast cancer metastasis: axillary lymph nodes, lungs, liver, and bone marrow [11–13]. Furthermore, overexpression of CXCR4 and/or SDF-1 has been correlated to worsened prognosis and disease-free survival [14–17]. Because CXCR4 plays an important role in the malignancy/metastasis of cancer, it is considered a candidate biomarker for evaluating cancer progression and perhaps the selection/monitoring of treatment strategies.

Recently, a lot of effort has been conducted in the development of CXCR4-specific antagonistic peptides. Small peptides, such as T140 and its derivative Ac-TZ14011, were selected based on their

Address all correspondence to: Fijs W.B. van Leeuwen, PhD, The Netherlands Cancer Institute, Plesmanlaan 121, 1066CX Amsterdam, the Netherlands.
E-mail: fw.v.leeuwen@nki.nl
[1]This research is supported by a KWF translational research award (grant no. PGF 2009-4344 to F.v.L.) and FP7-HYPERImage (grant no. 201651 to T.B.).
[2]This article refers to supplementary materials, which are designated by Table W1 and Figure W1 and are available online at www.transonc.com.
[3]Authors contributed equally.
Received 4 February 2011; Revised 23 February 2011; Accepted 2 March 2011

1944-7124/11
DOI 10.1593/tlo.11115

antagonistic properties toward the CXCR4 receptor and their potential for treatment. These and several other peptide derivatives have been used to reduce cell proliferation and migration *in vitro* and to cause inhibition of primary tumor growth and tumor metastasis *in vivo* [18–23]. A useful property of the Ac-TZ14011 peptide is that it has one free lysine group situated at a significant distance from the pharmacophore allowing functionalization with a single diagnostic antenna. For example, an ^{111}In-labeled DTPA-Ac-TZ14011–derivative has shown potential during the noninvasive imaging of the CXCR4 expression *in vivo* [23,24].

Because CXCR4 is part of a family of membrane-bound G protein–coupled receptors, staining of the cell surface membrane could be considered most representative. However, immunohistochemistry (IHC) on breast cancer tissue using antibodies directed against CXCR4 has shown staining of the cell surface membrane, the cytoplasm, and the nucleus of the cell [12–16,25]. Such differences between IHC localization and its natural role may present actual changes in the localization of CXCR4 or may be caused by the staining techniques used. Another downside of using antibodies for IHC is that the agent used for detection will differ from the peptides used *in vivo*.

Ideally, *ex vivo* validation is performed using a detection agent that accurately resembles the compound used for imaging. Nishizawa et al. [26] have demonstrated the value of the fluorescein-labeled T140 derivative TY14003 in the detection of high-grade bladder cancer. Hence, we reasoned that a fluorescent derivative of Ac-TZ14011 [27] can also potentially be used for fluorescent IHC (FIHC) of breast tumor tissue.

We here report on the use of the Ac-TZ14011–fluorescein isothiocyanate (FITC) peptide for FIHC of CXCR4-overexpressing cells/tumors. In this study, we compared its efficacy in detecting CXCR4 expression to that of the commercially available anti-CXCR4 antibodies.

Materials and Methods

Cell Culture

Human breast cancer cell lines MDAMB231 and MDAMB231^{CXCR4+} were kindly provided by Olaf van Tellingen and Ed Roos (NKI-AvL, Amsterdam, the Netherlands), respectively. MDAMB231^{CXCR4+} cells express higher levels of CXCR4 expression and have been selected using flow cytometry. MDAMB231 cells were used as control based on their basal CXCR4 expression. Both cell lines were maintained in Gibco's minimum essential medium enriched with 10% fetal bovine serum, penicillin, streptomycin L-glutamine, nonessential amino acids, sodium pyruvate, and minimum essential medium vitamins solution (Life Technologies Inc, Breda, the Netherlands). Cells were kept under standard culture conditions.

Flow Cytometry

Cell staining. Freshly cultured MDAMB231 or MDAMB231^{CXCR4+} cells were trypsinized, washed with 0.1% bovine serum albumin in phosphate-buffered saline (0.1% BSA/PBS) and then incubated for 1 hour with monoclonal phycoerythrin (PE) labeled anti-CXCR4 antibody (12G5-PE (1:5) or 2B11-PE (1:100); BD Biosciences, Breda, the Netherlands) or with Ac-TZ14011–FITC (1:200; for the preparation of Ac-TZ14011–FITC, see Supporting Information). Cells were labeled on ice or at room temperature (RT). After incubation, cells were washed with 0.1% BSA/PBS, and 5 minutes before analysis, propidium iodide (PI; 1:10000; BD Biosciences) was added to distinguish live and dead cells.

For fixed cell conditions, cells were trypsinized, washed with 0.1% BSA/PBS, and fixed with formalin overnight, again washed with 0.1% BSA/PBS, and then for 1 hour incubated with 12G5-PE, 2B11-PE, or Ac-TZ14011–FITC on ice, followed by washing with 0.1% BSA/PBS.

Peptides and antibodies were diluted in 0.1% BSA/PBS in all flow cytometry experiments. Non–antibody/peptide–incubated cells served as controls.

SDF-1 and Ac-TZ14011 competition experiment. One hour before the start of the experiment, MDAMB231 or MDAMB231^{CXCR4+} cells were given fresh culture medium. After trypsinization, 6.0×10^6 cells/ml were incubated for 1 hour on ice with 12G5-PE and SDF-1 (8.87 nM), Ac-TZ14011–FITC and SDF-1 (0.67 μM) or Ac-TZ12011–FITC and unlabeled Ac-TZ14011 (0.67 and 6.70 μM, respectively). Cells were washed with 0.1% BSA/PBS, PI was added, and cells were analyzed.

CXCR4 chemokine receptor expression-level determination using FACS. After staining, cells were analyzed using a Beckton Dickinson FACSCalibur (BD Biosciences) equipped with Cell Quest Pro software (BD Biosciences). FITC fluorescence was detected in the FL1 channel (excitation, 488 nm; emission filter, 530/30 nm). PE fluorescence was detected in the FL2 channel (excitation, 488 nm; emission filter, 585/42 nm). PI was detected in the FL3 channel (excitation, 488 nm; emission filter, >670 nm).

Mean fluorescent signal intensity ratios (MFIRs) were calculated as: (mean fluorescent signal intensity signal antibody or peptide incubated condition) / (mean fluorescent signal intensity control condition). To determine statistical significance between the different cell lines (Table 1) or the different incubation conditions (Tables 2 and W1), a standard *t* test was performed. All experiments were performed at least in triplicate.

Generation of Mouse Tumor Models

Before injection *in vivo*, cells were washed three times with Hanks buffered salt solution (Life Technologies Inc) and resuspended

Table 1. CXCR4 Expression on MDAMB231 and MDAMB231^{CXCR4+} Cells Incubated at Different Conditions (n = 3-6).

	Cell Type		Signal Intensity Difference MDAMB231 and MDAMB231^{CXCR4+}
	MDAMB231 MFIR ± SD	MDAMB231^{CXCR4+} MFIR ± SD	
12G5-PE			
Live cells; on ice	1.116 ± 0.054	4.920 ± 1.463	4.4*
Live cells; RT	1.160 ± 0.108	8.747 ± 1.245	7.5†
Fixed cells; on ice	7.380 ± 3.573	11.046 ± 2.143	1.5
2B11-PE			
Live cells; on ice	1.179 ± 0.072	1.487 ± 0.051	1.3†
Live cells; RT	1.206 ± 0.047	1.435 ± 0.042	1.2†
Fixed cells; on ice	18.814 ± 6.636	13.378 ± 3.267	0.7
Ac-TZ14011–FITC			
Live cells; on ice	2.337 ± 0.341	5.505 ± 0.900	2.4†
Live cells; RT	2.970 ± 0.289	4.941 ± 0.487	1.7*
Fixed cells; on ice	25.788 ± 1.575	62.357 ± 7.920	2.4†

For significance: MDAMB231 MFIRs were compared to MDAMB231^{CXCR4+} MFIRs.
*$P \leq .05$.
†$P \leq .005$.

Table 2. Antagonistic Ac-TZ14011–FITC Competes with SDF-1 and Ac-TZ14011 for the CXCR4 Receptor (n = 3).

	Cell Type			
	MDAMB231		MDAMB231^{CXCR4+}	
	MFIR ± SD	%	MFIR ± SD	%
12G5-PE	1.134 ± 0.033		2.186 ± 0.048	
SDF-1 + 12G5-PE	1.174 ± 0.009	+3	2.015 ± 0.080	−8
Ac-TZ14011–FITC	1.900 ± 0.049		6.905 ± 0.174	
SDF-1 + Ac-TZ14011–FITC	2.010 ± 0.044	+6	4.643 ± 0.339	−33*
Ac-TZ14011 + Ac-TZ14011–FITC	2.266 ± 0.095	+19†	2.985 ± 0.291	−57*

For significance: 12G5-PE/Ac-TZ14011–FITC MFIRs were compared to MFIRs of SDF-1/unlabeled Ac-TZ14011 + 12G5-PE/Ac-TZ14011–FITC incubated conditions.
% indicates percentage change in fluorescent signal intensity.
*$P \leq .005$.
†$P \leq .05$.

in Hanks buffered salt solution to a final concentration of 50.0 × 10^7 cells/ml and kept on ice.

Female BALB/c nude mice, 6 to 8 weeks old, were anesthetized with a mixture of hypnorm (Vetapharma, Leeds, United Kingdom), dormicum (Roche Diagnostics GmbH, Mannheim, Germany), and water suitable for injection (1:1:2; 5 μl/g intraperitoneally). MDAMB231 or MDAMB231^{CXCR4+} cells (1.0 × 10^6) were orthotopically injected into the left inguinal mammary fat pad. Because CXCR4 expression in the lymph nodes is intrinsically high, the left inguinal lymph node was cleared before injection of the tumor cells, hereby creating a low-background niche for the tumor cells to grow in. At 6 to 8 weeks after transplantation, mice were killed, and primary tumors (~4 cm^3) were taken out (n = 20). Hereafter, fresh tumor tissue could be analyzed, or the tumor tissue was formalin-fixed and paraffin-embedded and used for IHC and FIHC.

All animal experiments were performed in accordance with Dutch animal welfare regulations and approved by the local ethics committee.

Immunohistochemistry

Formalin-fixed paraffin-embedded MDAMB231 or MDAMB231^{CXCR4+} tumor tissue sections, 4 μm in size, were deparaffinized. Sections were heated for 30 minutes at 95°C in citrate buffer (pH 6) to retrieve antigenic activity, followed by 30 minutes cooling at RT. For antibody 12G5, slides were incubated for 30 minutes with protein kinase or 20 minutes with trypsin at 37°C or heated for 30 minutes at 95°C in Tris/EDTA (pH 9) followed by 30 minutes cooling at RT. Slides were rinsed with PBS and incubated overnight at 4°C with a monoclonal anti–CXCR4-antibody (clone 2B11 [1:100; n = 5-10] or clone 12G5 [1:100; n = 3]; BD Biosciences). After washing, slides were incubated for 1 hour at RT with the secondary antibody, goat-anti-rat (sc-2041; 1:100; Santa Cruz Technology, Heidelberg, Germany) or with goat-anti-mouse (E0433; 1:500; DAKO, Glostrup, Denmark) for clones 2B11 and 12G5, respectively. Negative controls were only incubated with the secondary antibody. Slides were then washed and incubated for 30 minutes with horseradish peroxidase–labeled streptavidin-biotin complex (1:200; DAKO). Slides were developed with 3,3′-diamobenzidine tetrahydrochloride (Sigma-Aldrich, Zwijndrecht, the Netherlands) and slightly counterstained with hematoxylin (Sigma-Aldrich). Images were taken with a color CCD microscope system (Axiovert S100 with AxioCam HRc; Carl Zeiss BV, Sliedrecht, the Netherlands) and analyzed using AxioVision (Carl Zeiss).

Confocal Imaging

Fluorescent immunohistochemistry of formalin-fixed paraffin-embedded tumor tissue. After deparaffinization, antigen retrieval incubation, and three PBS washes (as described in the IHC section), slides were incubated for 1 hour at RT with Ac-TZ14011–FITC (1:200; n = 3). Thereafter, slides were washed with PBS, counterstained with 4′,6-diamidine-2′-phenylindole dihydrochloride (DAPI; 1:1000; Roche Diagnostics GmbH) and washed thoroughly. Negative controls were only incubated with DAPI. Slides were mounted with Vectashields mounting medium for fluorescence to preserve the fluorescent signal (Vector Laboratories Inc, Burlingame, CA).

In vitro *immunofluorescence.* Before the start of the experiment, 1.0 × 10^5 MDAMB231 and MDAMB231^{CXCR4+} cells were seeded at coverslips (Ø 24 mm; Karl Heicht GmbH&Co, Sondheim, Germany). After 24 to 48 hours (80% confluency), cells were washed with PBS and incubated for 1 hour on ice or at RT with Ac-TZ14011–FITC (1:200) and washed again with ice-cold PBS. Cells were stored in PBS on ice until analysis. For the internalization experiment, images were taken 15, 30, and 60 minutes after the t = 0 image was taken. Cells were warmed with RT PBS.

For fixed cell conditions, cells were placed in formalin overnight, washed with PBS, and then incubated for 1 hour on ice with Ac-TZ14011–FITC. After washing with ice-cold PBS confocal images were taken. Non–peptide-incubated slides served as negative control.

Ex vivo *fluorescent tumor tissue imaging*. MDAMB231 or MDAMB231^{CXCR4+} tumor-bearing mice were killed, and excised tumor tissue was formalin-fixed for 24 hours (n = 3). After slicing, tissue was incubated for 1 hour with Ac-TZ14011–FITC (1:200) followed by PBS washes and incubation with DAPI (1:1000) for 10 minutes and again thoroughly washed with ice-cold PBS.

Results

In the present study, we investigated the use of a FITC-labeled antagonistic CXCR4 peptide, Ac-TZ14011–FITC, in direct fluorescence-based visualization of the CXCR4 expression levels in MDAMB231 and MDAMB231^{CXCR4+} cells and tumors derived thereof.

Determination of the Specificity of Ac-TZ14011–FITC for CXCR4

To make sure the synthesized antagonistic CXCR4 peptide (Ac-TZ14011–FITC) specifically stains CXCR4, its specificity was validated using flow cytometric analysis. MFIRs of MDAMB231 (low CXCR4 expression) and MDAMB231^{CXCR4+} (high CXCR4 expression) showed a 2.4 times (P = .0003) higher signal intensity on MDAMB231^{CXCR4+} cells compared with MDAMB231 cells when live cells were incubated on ice with Ac-TZ14011–FITC (Table 1). However, after incubation at RT, only a 1.7 times (P = .04) higher signal intensity could be detected on MDAMB231^{CXCR4+} cells (Table 1). PE-labeled anti-CXCR4 antibody clones 12G5 or 2B11 (referred to as 12G5-PE or 2B11-PE, respectively) were used as a reference staining. As can be seen in Table 1, after incubation with 12G5-PE, a 4.4 times higher MFIR (P = .01) could be detected in MDAMB231^{CXCR4+} cells compared with MDAMB231 cells. Incubation at RT resulted in a 7.5 times higher MFIR (P = .0012). For 2B11-PE, the measured difference in MFIR was only 1.3 times

(P = .003) and 1.2 times (P = .0035) higher when incubated on ice or at RT.

When formalin-fixed cells were stained with Ac-TZ14011–FITC for CXCR4, signal intensities and thereby the MFIRs increased for both MDAMB231 (MFIR 25.788 ± 1.575) and MDAMB231^{CXCR4+} (MFIR 62.357 ± 7.920) cells. However, the ratio between the two remained identical to that in live cells incubated on ice, namely, 2.4 (P < .0001). Significant differences could no longer be detected when formalin-fixed MDAMB231 and MDAMB231^{CXCR4+} cells were incubated with 12G5-PE (MFIRs 7.380 ± 3.573 and 11.046 ± 2.143, P = .22) or 2B11-PE (MFIRs 18.814 ± 6.636 and 13.378 ± 3.267, P = .29; Table 1).

SDF-1 Competition Experiment

To further determine the binding specificity and affinity of the Ac-TZ14011–FITC peptide for the CXCR4 receptor, an SDF-1 competition experiment was performed (Table 2). SDF-1 was added to occupy the CXCR4 receptors, hereby preventing Ac-TZ14011–FITC to bind to the receptor. In the presence of Ac-TZ14011–FITC and SDF-1, the MFIR decreased with 33% compared with MDAMB231^{CXCR4+} cells that were incubated with Ac-TZ14011–FITC alone (from 6.905 ± 0.174 to 4.643 ± 0.339, P = .002). A slight increase (6%) in MFIR was found when MDAMB231 cells were incubated with Ac-TZ14011–FITC and SDF-1 (from 1.900 ± 0.049 to 2.010 ± 0.044, P = .17). Coincubation of 12G5-PE and SDF-1 resulted in an 8% decrease of MFIR in MDAMB231^{CXCR4+} (from 2.186 ± 0.480 to 2.015 ± 0.080, P = .13), where the MFIR of MDAMB231 cells increased with 3% (from 1.134 ± 0.033 to 1.174 ± 0.009, P = .29). For blocking experiments with SDF-1, see Supporting Information.

Ac-TZ14011 Competition Experiment

Competition with the parental Ac-TZ14011 peptide was used to underline the specificity of Ac-TZ14011–FITC. When cells were coincubated with an excessive amount of unlabeled Ac-TZ14011 and Ac-TZ14011–FITC, the MFIR of MDAMB231^{CXCR4+} cells decreased with 57% (from 6.905 ± 0.174 to 2.985 ± 0.291, P = .0041). The MFIR of MDAMB231 cells increased with 19% (from 1.900 ± 0.049 to 2.266 ± 0.095, P = .0095).

Ac-TZ14011–FITC Distribution in Cultured Tumor Cells

Confocal images help to determine the cellular localization of Ac-TZ14011–FITC after binding to the cells. As Figure 1*A* shows, on MDAMB231 cells, (i) only a faint membranous staining could be detected. In MDAMB231^{CXCR4+} cells, a much higher degree of membranous staining could be detected (ii). Where initial staining was predominantly membranous, images taken over time (t = 0-60 min; Figure 1*C*) revealed progressive internalization of the fluorescent signal into the cell. Here, endocytosis resulted in internalization of Ac-TZ14011–FITC in vesicle-like structures visible in the cytoplasm.

Incubation on ice of formalin-fixed cells with Ac-TZ14011–FITC yielded an entirely different staining pattern. Ac-TZ14011–FITC was found throughout the entire cell, in both MDAMB231 (Figure 1*Bi*) and MDAMB231^{CXCR4+} (Figure 1*Bii*) cells. However, the staining in MDAMB231^{CXCR4+} cells was more intense than that of MDAMB231 cells.

Ac-TZ14011–FITC for FIHC

Standard IHC was performed to determine the CXCR4 expression in tumor tissue. Using the 12G5 antibody, only a minor degree of staining could be detected in the MDAMB231 tumor tissue. MDAMB231^{CXCR4+} tumor tissue, however, stained brownish all over but no clear cytoplasmatic or membranous staining could be discriminated. Because the control tissue (only incubated with secondary antibody) showed a similar staining pattern (data not shown), these results were deemed nonspecific. Different antigen retrieval steps were evaluated, but this did not reveal in any specific staining of the tissue (data not shown).

Incubation of MDAMB231^{CXCR4+} tissue with the 2B11 antibody resulted in strongly positively stained regions. In these regions, both membranous and cytoplasmatic staining could be detected (Figure 2*Bii*). In comparison, little to no staining was detected on MDAMB231 tumor tissue (Figure 2*Bi*). The negative control slides showed no nonspecific staining.

To our surprise, deparaffinized MDAMB231 tumor tissue incubated with Ac-TZ14011–FITC showed strong nonspecific staining in the nuclear membrane, nucleoli, and connective tissue (Figure 2*Ci*). MDAMB231^{CXCR4+} tumor tissue slides, however, showed a somewhat different staining profile with predominantly cytoplasmatic and membranous staining (Figure 2*Cii*).

When tumor tissue was not paraffin-embedded but only formalin-fixed for 24 hours, Ac-TZ14011–FITC staining of MDAMB231^{CXCR4+} tumor tissue (Figure 2*Dii*) was much more intense compared with MDAMB231 tumor tissue (Figure 2*Di*). This result is in line with the difference in staining intensity observed with 2B11 (Figure 2, *Bi* and *ii*). However, as can be seen in Figure 2, *Di* and *ii*, staining was detected throughout the entire cell, and staining was not confined to the membrane and cytoplasm. This staining pattern in fixed tissue is highly similar to that observed in fixed cells (see above Figure 1*Bi* and *ii*). For tumor staining patterns after intravenous administration of Ac-TZ14011–FITC, see the Supporting Information.

Discussion

Both for therapeutic and diagnostic applications, pathology, or rather IHC, is considered the standard in determination of the CXCR4 expression levels in tumor tissue. In this study, we investigated the potential of the fluorescent peptide Ac-TZ14011–FITC in fluorescence-based detection of CXCR4 expression levels. Other than conventional antibody-based IHC procedures, this fluorescent derivative of Ac-TZ14011 may, in the future, be used to visualize exactly the same features at FIHC as can be detected in noninvasive single-photon emission computed tomography imaging using the radioactive derivative ^{111}In-DTPA-Ac-TZ14011.

A discussion regarding the use of CXCR4-overexpressing cell lines rather than CXCR4-transfected cell lines is provided in the Supporting Information section.

CXCR4 Affinity of Ac-TZ14011–FITC

After validating the ability of Ac-TZ14011–FITC to discriminate between MDAMB231 and MDAM231^{CXCR4+} cells (Table 1), the affinity of Ac-TZ14011–FITC for CXCR4 was further validated with competition (and blocking) experiments. Competition with SDF-1 gave a 33% reduction in peptide binding to the MDAM231^{CXCR4+} cells (Table 2). Blocking gave a 29% reduction (Table W1). It can be concluded that SDF-1 has a higher affinity for CXCR4 than Ac-TZ14011–FITC, which is in accordance with results found by Nomura et al. [28]. For the antibody 12G5-PE, we were not able to induce a significant reduction in uptake during a competition experiment with SDF-1, suggesting both can simultaneously interact with CXCR4.

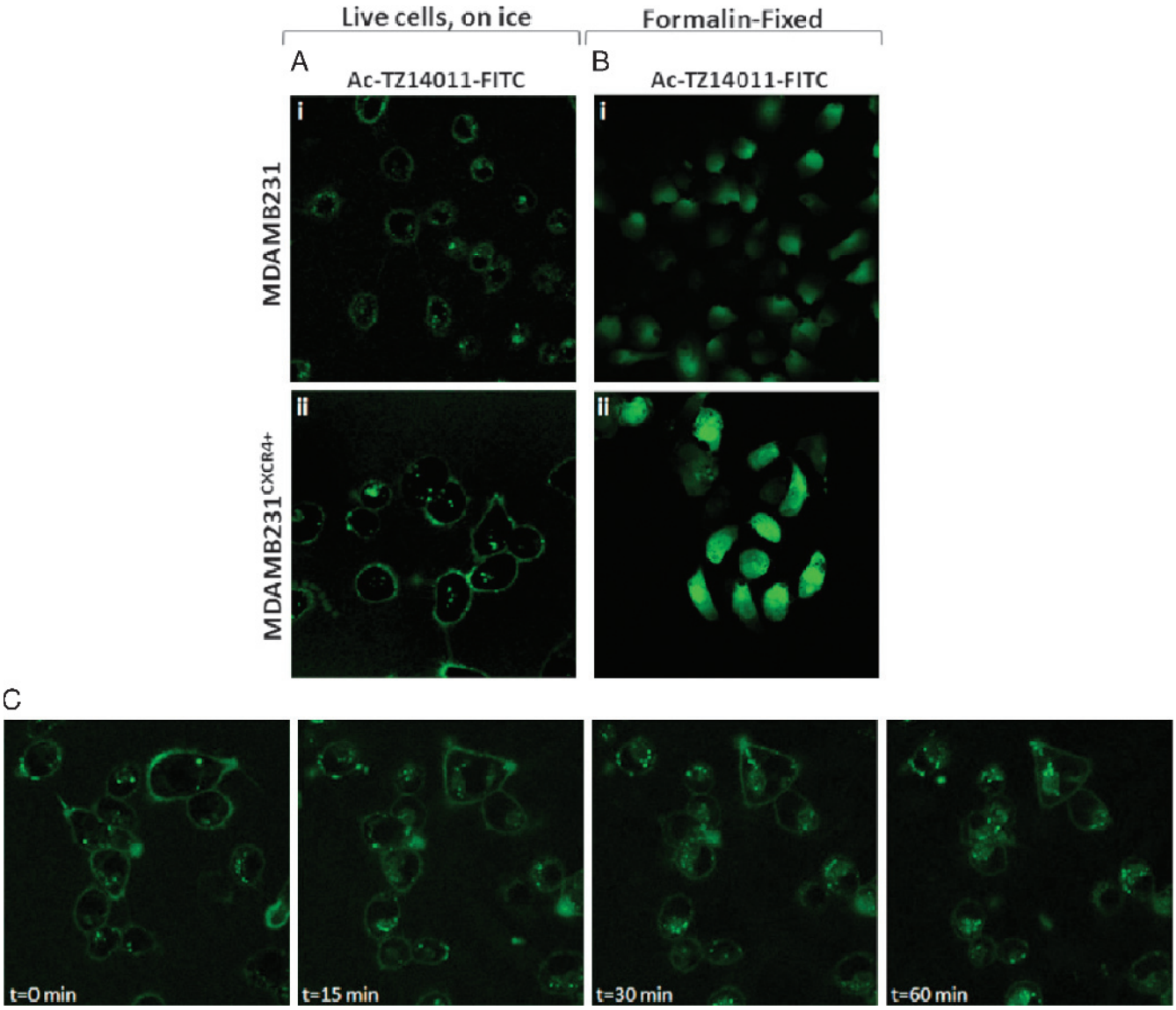

Figure 1. Ac-TZ14011–FITC distribution in live and formalin-fixed MDAMB231 and MDAMB231^{CXCR4+} tumor cells. (A) Live MDAMB231 and MDAMB231^{CXCR4+} cells were incubated with Ac-TZ12011–FITC for 1 hour on ice. (B) Formalin-fixed cells were incubated for 1 hour with Ac-TZ12011–FITC on ice. (C) MDAMB231^{CXCR4+} cells were incubated for 1 hour with Ac-TZ12011–FITC on ice, and confocal images were taken (t = 0 minute). Over time, Ac-TZ12011–FITC-CXCR4 receptor complexes internalized via vesicles (t = 0–60 minutes). Original magnification, ×630.

Experiments with the "low" CXCR4-expressing MDAM231 cells show an increase in peptide binding (Tables 2 and W1), of which only the 19% obtained after coincubation with an excess of Ac-TZ14011 is significant. Most likely, the high extracellular concentration of Ac-TZ14011 drives nonspecific uptake, also resulting in an increase in uptake of the structurally very similar Ac-TZ14011–FITC derivative. This effect, however, does not seem to dominate in the MDAM231^{CXCR4+} cells.

Cellular Localization of CXCR4

Using different antibodies, positive staining of the cell membrane, the cytoplasm, and even the nucleus has been reported [10,12–16,29,30]. However, as previously mentioned by Fischer et al. [29] and Kryczek et al. [30], nuclear localization would not be compatible with CXCR4 being a membrane receptor and its function in cancer cell migration and homing. Hence, membranous staining is considered most representative. Identical with the results published by Nomura et al. [28] and Zhang et al. [31], we found that Ac-TZ14011–FITC predominantly binds to CXCR4 on the cell membrane (Figure 1*A*) when live cells were incubated with Ac-TZ14011–FITC. Furthermore, membrane Ac-TZ14011–FITC-CXCR4 complexes internalized into the cell in small cytoplasmic vesicles (Figure 1*C*) [28,31]. Ac-TZ14011–FITC distribution throughout the entire cell was only observed when fixed cells or tissues were incubated. These results suggest fixation may influence the distribution of the staining agent.

Viable versus *Fixed Material*

Confocal images helped resolve questions about the difference in signal intensity seen with flow cytometry between live and fixed cells (Figure 1 and Table 1). The distribution of Ac-TZ14011–FITC in fixed cells, wherein the whole cell was stained, was completely different from the distribution observed in viable cells. Formalin slightly

permeabilizes the cell membranes, which might induce cellular and nuclear uptake of Ac-TZ14011–FITC. Although the fixed cells stained positive all over, the staining intensity of MDAMB231^{CXCR4+} cells was more intense than seen in MDAMB231 cells, which is in accordance with the results obtained with flow cytometry (Table 1). Fixation artifacts may also be of influence on the distribution patterns observed at IHC, and the latter may thus not accurately represent the CXCR4 expression patterns in viable tissue.

In addition to fixation, paraffinization also had a negative influence on the peptide-based staining (Figure 2*C*). A clear differentiation could, however, be made on only formalin-fixed tissue (Figure 2*D*).

Antibodies versus *Peptides*

During this study, anti-CXCR4 antibody clones 12G5 and 2B11 were used as reference. These antibodies differ in the "type" of CXCR4 that they recognize; where antibody 12G5 is directed against human origin CXCR4, antibody 2B11 is directed toward murine CXCR4. In flow cytometry of viable cells, the 12G5-PE antibody was able to nicely distinguish MDAMB231 from MDAMB231^{CXCR4+} cells, whereas the 2B11-PE antibody did not perform as well (Table 1). However, when the cells were fixed, neither of the antibodies was able to distinguish between the two cell lines. Surprisingly, in IHC, an opposite effect was observed; anti-murine 2B11 antibody gave specific staining on the human-originated MDA tumors, whereas anti-human 12G5 antibody did not (Figure W1, *Ai* and *ii*). This observation underlines that antibodies are not always interchangeable between different detection viz. flow cytometry and IHC, whereas Ac-TZ14011–FITC peptide can be used in both cases.

To overcome both the need of using different antibodies for flow cytometry and IHC staining, Ac-TZ14011–FITC can be used. This peptide showed corresponding results in studies on cells and tumor tissue (Table 1 and Figures 1*B* and 2*D*). Clearly, this will be most beneficial for evaluation of the more "experimental" biomarkers such as CXCR4 and in combination with multispectral FIHC that allows for the simultaneous detection of multiple biomarkers at once.

The main advantage of using peptides for IHC visualization of CXCR4 is that it makes it easier to directly correlate IHC stainings with imaging findings obtained using the ^{111}In-DTPA-Ac-TZ14011 analog. Such a combination of differently labeled derivatives of the same peptide sequence would improve the integration of *in vitro* and *in vivo* diagnostics. Of course, a similar approach may be achieved using a combination of, for example, ^{125}I-12G5 and 12G5-PE [32]. However, using an antibody takes away the advantages small molecules such as peptides have. Moreover, it would make it more difficult to measure/predict therapy response based on treatment with CXCR4-inhibitory peptides.

Signal intensity differences obtained in flow cytometry varied between 12G5-PE and Ac-TZ14011–FITC (Table 1). While the latter shows significant differences under all the conditions studied, 12G5-PE showed larger differences between the live conditions studied in MDAMB231 and MDAMB231^{CXCR4+} cells. This result suggests that, with Ac-TZ14011–FITC, there is somewhat more nonspecific cellular uptake than with 12G5-PE.

Ex Vivo *Visualization of CXCR4 Expression in Tumor Tissue*

During *ex vivo* (F)IHC, the peptide/antibody has access to the whole tumor tissue slide and, therefore, is able to stain all CXCR4

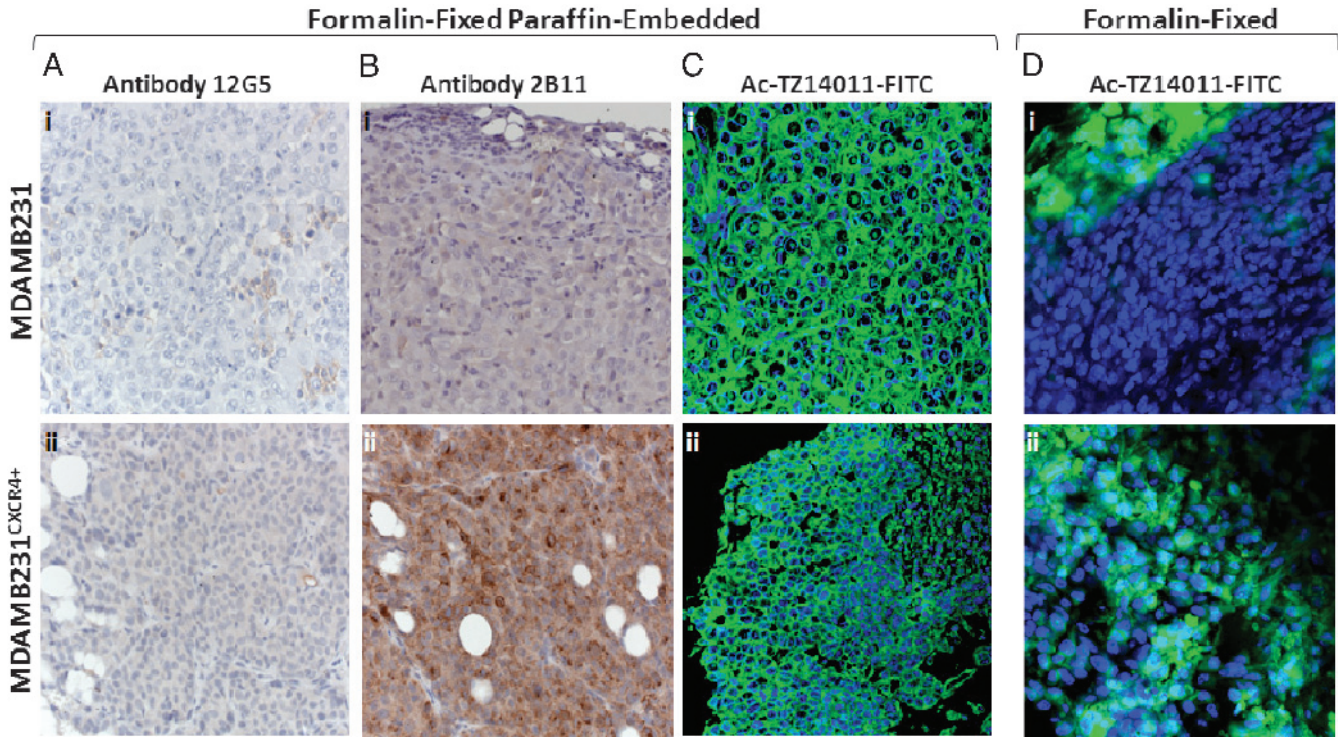

Figure 2. Predominant cytoplasmatic CXCR4 expression on formalin-fixed paraffin-embedded and freshly isolated, formalin-fixed, breast cancer tissue. (A) Formalin-fixed paraffin-embedded slides were incubated with the primary anti-CXCR4 antibody clone 12G5, (B) primary anti-CXCR4 antibody clone 2B11 (original magnification, ×400; n = 5-10), or (C) incubated with Ac-TZ12011–FITC (original magnification, ×630; n = 3). (D) Freshly isolated, formalin-fixed tumor tissue incubated with Ac-TZ12011–FITC showed a different staining pattern. Original magnification, ×630; n = 3.

present. Intravenously administrated Ac-TZ14011–FITC (see Supporting Information) predominantly has access to the blood supplied areas of the tumor and will only provide a specific signal after binding of extracellular expressed CXCR4 (Figures 1*C* and W1*B*). Hence, this only gave local staining. The intravenous incubation demonstrates how Ac-TZ14011-FITC can visualize the staining efficacy that would be achieved using the molecular imaging agent ^{111}In-DTPA-Ac-TZ14011. This application illustrates how the Ac-TZ14011 peptide (and perhaps many others), in combination with different diagnostic "antennae," can, in the future, be used to directly correlate *in vivo* findings with *ex vivo* stainings.

Conclusions

In conclusion, the present study illustrates the value of Ac-TZ14011–FITC to identify tumor cells with slightly upregulated CXCR4 expression levels. The fluorescent peptide antagonist can be used during both FIHC and flow cytometry. Where results with antibodies rely on employment of different antibodies for different applications, Ac-TZ14011–FITC is widely applicable. The peptide application in FIHC broadens the diagnostic application of Ac-TZ14011 from a use *in vitro*, *in vivo*, and now even *ex vivo*.

Acknowledgments

The authors thank Ed Roos for critically reviewing the article. The authors also thank the members of the Animal Pathology, Digital Microscopy, and the Flow Cytometry facility for their help.

References

[1] Donzella GA, Schols D, Lin SW, Esté JA, Nagashima KA, Maddon PJ, Allaway GP, Sakmar TP, Henson G, De Clercq E, et al. (1998). AMD3100, a small molecule inhibitor of HIV-1 entry via the CXCR4 co-receptor. *Nat Med* **4**(1), 72–77.

[2] Tarasova NI, Stauber RH, and Michejda CJ (1998). Spontaneous and ligand-induced trafficking of CXC-chemokine receptor 4. *J Biol Chem* **273**(26), 15883–15886.

[3] Balkwill F (2004). Cancer and the chemokine network. *Nat Rev Cancer* **4**(7), 540–550.

[4] Nanki T, Hayashida K, El-Gabalawy HS, Suson S, Shi K, Girschick HJ, Yavuz S, and Lipsky PE (2000). Stromal cell–derived factor 1—CXC—chemokine receptor 4 interactions play a central role in CD4$^+$ T-cell sccumulation in rheumatoid arthritis synovium. *J Immunol* **165**(11), 6590–6598.

[5] Nanki T, Takada K, Komano U, Morio T, Kanegane H, Nakajima A, Lipsky PE, and Miyasaka N (2009). Chemokine receptor expression and functional effects of chemokines on B cells: implication in the pathogenesis of rheumatoid arthritis. *Arthritis Res Ther* **11**(5), R149.

[6] Andreas K, Lübke C, Häupl T, Dehne T, Morawietz L, Ringe J, Kaps C, and Sittinger M (2008). Key regulatory molecules of cartilage destruction in rheumatoid arthritis: an *in vitro* study. *Arthritis Res Ther* **10**(1), R9.

[7] Kang H, Watkins G, Douglas-Jones A, Mansel RE, and Jiang WG (2005). The elevated level of CXCR4 is correlated with nodal metastasis of human breast cancer. *Breast* **14**, 360–367.

[8] Balkwill F (2004). The significance of cancer cell expression of the chemokine receptor CXCR4. *Semin Cancer Biol* **14**(3), 171–179.

[9] Kulbe H, Levinson NR, Balkwill F, and Wilson JL (2004). The chemokine network in cancer—much more than directing cell movement. *Int J Dev Biol* **48**(5–6), 489–496.

[10] Arya M, Ahmed H, Silhi N, Williamson M, and Patel HRH (2007). Clinical importance and therapeutic implications of the pivotal CXCL12-CXCR4 (chemokine ligand-receptor) interaction in cancer cell migration. *Tumor Biol* **28**(3), 123–131.

[11] Müller A, Homey B, Soto H, Ge N, Catron D, Buchanan ME, McClanahan T, Murphy E, Yuan W, Wagner SN, et al. (2001). Involvement of chemokine receptors in breast cancer metastasis. *Nature* **410**(6824), 50–56.

[12] Woo SU, Bae JW, Kim CW, Lee JL, and Koo BW (2008). A significant correlation between nuclear CXCR4 expression and axillary lymph node metastasis in hormonal receptor negative breast cancer. *Ann Surg Oncol* **15**(1), 281–285.

[13] Andre F, Xia W, Conforti R, Wei Y, Boulet T, Tomasic G, Spielmann M, Zoubir M, Berrada N, Arriagada R, et al. (2009). CXCR4 expression in early breast cancer and risk of distant recurrence. *Oncologist* **14**(12), 1182–1188.

[14] Kato M, Kitayama J, Kazama S, and Nagawa H (2003). Expression pattern of CXC chemokine receptor-4 is correlated with lymph node metastasis in human invasive ductal carcinoma. *Breast Cancer Res* **5**(5), R144–R150.

[15] Mirisola V, Zuccarino A, Bachmeier BE, Sormani MP, Falter J, Nerlich A, and Pfeffer U (2009). CXCL12/SDF1 expression by breast cancers is an independent prognostic marker of disease-free and overall survival. *Eur J Cancer* **45**(14), 2579–2587.

[16] Kang H, Watkins G, Parr C, Douglas-Jones A, Mansel RE, and Jiang WG (2005). Stromal cell derived factor-1: its influence on invasiveness and migration of breast cancer cells *in vitro*, and its association with prognosis and survival in human breast cancer. *Breast Cancer Res* **7**(4), R402–R410.

[17] Huang X, Shen J, Cui M, Shen L, Luo X, Pei G, Jiang H, and Chen K (2003). Molecular dynamics simulations on SDF-1α: binding with CXCR4 receptor. *Biophys J* **84**, 171–184.

[18] Trent JO, Wang Z, Murray JL, Shao W, Tamamura H, Fujii N, and Peiper SC (2003). Lipid bilayer simulations of CXCR4 with inverse agonists and weak partial agonists. *J Biol Chem* **278**(47), 47136–47144.

[19] Zhang W, Navenot JM, Haribabu B, Tamamura H, Hiramatu K, Omagari A, Pei G, Manfredi JP, Fujii N, Broach JR, et al. (2002). A point mutation that confers constitutive activity to CXCR4 reveals that T140 is an inverse agonist and that AMD3100 and ALX40-4C are weak partial agonists. *J Biol Chem* **277**(27), 24515–24521.

[20] Tamamura H, Omagari A, Oishi S, Kanamoto T, Yamamoto N, Peiper SC, Nakashima H, Otaka A, and Fujii N (2000). Pharmacophore identification of a specific CXCR4 inhibitor, T140, leads to development of effective anti-HIV agents with very high selectivity indexes. *Bioorg Med Chem Lett* **10**(23), 2633–2637.

[21] Liang Z, Wu T, Lou H, Yu X, Taichman RS, Lau SK, Nie S, Umbreit J, and Shim H (2004). Inhibition of breast cancer metastasis by selective synthetic polypeptide against CXCR4. *Cancer Res* **64**(12), 4302–4308.

[22] Huang EH, Singh B, Cristofanilli M, Gelovani J, Wei C, Vincent L, Cook KR, and Lucci A (2009). A CXCR4 antagonist CTCE-9908 inhibits primary tumor growth and metastasis of breast cancer. *J Surg Res* **155**(2), 231–236.

[23] Hanaoka H, Mukai T, Tamamura H, Mori T, Ishino S, Ogawa K, Iida Y, Doi R, Fujii N, and Saji H (2006). Development of 111-In-labeled peptide derivative targeting a chemokine receptor, CXCR4, for imaging tumors. *Nucl Med Biol* **33**(4), 489–494.

[24] Kuil J, Velders AH, and van Leeuwen FWB (2010). Multimodal tumor-targeting peptides functionalized with both a radio- and a fluorescent label. *Bioconjug Chem* **21**(10), 1707–1719.

[25] Li YM, Pan Y, Wei Y, Cheng X, Zhou BP, Tan M, Zhou X, Xia W, Hortobagyi GN, Yu D, et al. (2004). Upregulation of CXCR4 is essential for HER2-mediated tumor metastasis. *Cancer Cell* **6**(5), 459–469.

[26] Nishizawa K, Nishiyama H, Oishi S, Tanahara N, Kotani H, Mikami Y, Toda Y, Evans BJ, Peiper SC, Saito R, et al. (2010). Fluorescent imaging of high-grade bladder cancer using a specific antagonist for chemokine receptor CXCR4. *Int J Cancer* **127**, 1180–1187.

[27] Oishi S, Masuda R, Evans B, Ueda S, Goto Y, Ohno H, Hirasawa A, Tsujimoto G, Wang Z, Peiper SC, et al. (2008). Synthesis and application of fluorescein- and biotin-labeled molecular probes for the chemokine receptor CXCR4. *Chembiochem* **9**, 1154–1158.

[28] Nomura W, Tanabe Y, Tsutsumi H, Tanaka T, Ohba K, Yamamoto N, and Tamamura H (2008). Fluorophore labeling enables imaging and evaluation of specific CXCR4-ligand interaction at the cell membrane for fluorescence-bases screening. *Bioconjug Chem* **19**(9), 1917–1920.

[29] Fischer T, Nagel F, Jacobs S, Stumm R, and Schultz S (2008). Reassessment of CXCR4 chemokine receptor expression in human normal and neoplastic tissues using the novel rabbit monoclonal antibody UMB-2. *PLoS One* **3**(12), e4069.

[30] Kryczek I, Wei S, Keller E, Liu R, and Zou W (2007). Stromal-derived factor (SDF-1/CXCL12) and human tumor pathogenesis. *Am J Physiol Cell Physiol* **292**(3), C987–C995.

[31] Zhang Y, Foudi A, Geay JF, Berthebaud M, Buet D, Jarrier P, Jalil A, Vainchenker W, and Louache F (2004). Intracellular localization and constitutive endocytosis of CXCR4 in human CD34$^+$ hematopoietic progenitor cells. *Stem Cells* **22**(6), 1015–1029.

[32] Nimmagadda S, Pullambhatla M, and Pomper MG (2009). Immunoimaging of CXCR4 expression in brain tumor xenografts using SPECT/CT. *J Nucl Med* **7**(50), 1124–1130.

Supporting Information

Methods

Ac-TZ14011–FITC synthesis. The antagonistic CXCR4 peptide, Ac-TZ14011, was synthesized as described previously [1]. A stock solution of Ac-TZ14011–FITC of 1 mg/ml in 5% ethanol in water was made. Aliquots of this stock were stored at −20°C and, when necessary, an aliquot was diluted before the experiment and the dilution factor is indicated for each experiment.

Fluorescein isothiocyanate isomer I (FITC; 2.32 mg, 5.95 μmol) in 500 μl of dimethyl sulfoxide was added to the antagonistic CXCR4 peptide (11.1 mg, 3.96 μmol) in 1 ml of 0.1 M $NaHCO_3$ (Merck, Schiphol-Rijk, the Netherlands) and 2 ml of CH_3CN (Acros, Geel, Belgium). The mixture was stirred overnight at RT, solvents were evaporated, and the product was purified by preparative high-performance liquid chromatography using a Waters HPLC system with a UV detector operating at 230 nm and a Waters Atlantis C18 10 μm (250 × 19 mm) column using a gradient of 0.05% trifluoroacetic acid (Sigma-Aldrich) in H_2O/CH_3CN 9:1 to 0.05% trifluoroacetic acid in H_2O/CH_3CN 1:4 in 40 minutes. A yellow fluffy solid (4.3 mg, 35%) was obtained after lyophilization of the pooled fractions and characterized by MALDI-TOF-MS.

The fluorescein-labeled CXCR4 peptide antagonist will be reverted to as Ac-TZ14011–FITC from here on. All experiments were performed in the absence of light when fluorescent labels were used.

Cell staining: SDF-1 block experiment. One hour before the start of the block experiment, MDAMB231 or MDAMB231^{CXCR4+} cells were given fresh culture medium. After trypsinization, 2.0×10^6 cells/ml were incubated for 1.5 hours at 37°C with 1.5 μg of SDF-1 (Peprotech via Bio Connect, Huissen, the Netherlands) in culture medium. SDF-1 was removed by centrifugation (5 min, 1200 rpm, 4°C), and cells were resuspended at 6.0×10^6 cells/ml before incubation on ice for 1 hour with 12G5-PE or Ac-TZ14011–FITC. Hereafter, cells were washed with 0.1% BSA/PBS, PI was added, and cells were analyzed.

Ex vivo *detection after intravenous administration of Ac-TZ14011–FITC.* In addition, MDAMB231 or MDAMB231^{CXCR4+} tumor-bearing mice were intravenously injected with 50 μg of Ac-TZ14011–FITC (n = 3). Twenty-four hours after injection, mice were killed, and tumors were excised and kept in PBS or formalin on ice. Then, thin slices were cut, washed with ice-cold PBS, incubated for 10 minutes with DAPI, and again thoroughly washed before images of the fresh tumor tissue were obtained. Furthermore, excised tumors were formalin fixed on ice for 3 hours, cut into thin slices, and washed with ice-cold PBS and incubated with DAPI before confocal images were obtained. Controls were only incubated with DAPI before imaging.

Confocal microscope properties. Confocal images were taken on a Leica TCS-SP2-AOBS live confocal microscope (Leica Microsystems Heidelberg, GmbH, Heidelberg, Germany; magnification, ×400/×630). DAPI was excited at 405 nm, and emission was detected between 409 and 468 nm. FITC was excited at 488 nm, and emission was detected between 510 and 585 nm. A Leica TCS-NT confocal microscope (Leica Microsystems Heidelberg GmbH; magnification, ×630) with Leica Confocal Software was used to analyze the MDAMB231 and MDAMB231^{CXCR4+} Ac-TZ14011–FITC–incubated tumor cells. Emission of FITC was detected between 510 and 585 nm. Pictures were captured, and overlays were made using Leica Confocal Software (Leica Microsystems Heidelberg GmbH).

Results

SDF-1 block experiment. On binding of SDF-1, the CXCR4 receptor internalizes and becomes cleared from the membrane [1,2]. To study this effect, MDAMB231^{CXCR4+} cells were preincubated for 1.5 hours with SDF-1 at 37°C. After removal of the excess SDF-1 in solution, cells were incubated with 12G5-PE or Ac-TZ14011–FITC for 1 hour on ice to determine the amount of CXCR4 left on the cell membranes. As can be seen in Table W1, preincubation of MDAMB231^{CXCR4+} cells with SDF-1 followed by Ac-TZ14011–FITC incubation revealed 29% decrease in MFIR compared with incubation with Ac-TZ14011–FITC alone (from 5.184 ± 0.144 to 3.699 ± 0.034, P = .0037). In addition, 14% less 12G5-PE was bound by MDAMB231^{CXCR4+} cells that were preincubated with SDF-1 followed by 12G5-PE incubation (MFIR decreased from 1.485 ± 0.018 to 1.274 ± 0.033, P = .0043), indicating that 14% of the CXCR4 receptors internalize after binding SDF-1.

The SDF-1 block experiment was not performed for MDAMB231 cells because these already show limited CXCR4 expression levels in the absence of SDF-1.

FIHC of tumors after intravenous Ac-TZ14011–FITC administration in mice. Alternative to *ex vivo* tissue incubation with Ac-TZ14011–FITC, this peptide can also be used for *in vivo* (intravenous) tumor staining. Mice bearing MDAMB231 or MDAMB231^{CXCR4+} tumors were intravenously injected with Ac-TZ14011–FITC. Tumors were excised after 24 hours wherein the tumor tissue was analyzed using a confocal microscope (a schematic overview is given in Figure W1*A*). After intravenous incubation, MDAMB231^{CXCR4+} tumor tissue slices regionally stained positive for CXCR4 (Figure W1*Bii*). Under these conditions, MDAMB231 tumor tissue (Figure W1*Bi*) hardly stained positive for CXCR4.

Formalin fixation of the Ac-TZ14011–FITC preincubated tissue still predominantly revealed cytoplasmic staining for CXCR4 on MDAMB231^{CXCR4+} tumor tissue slices (Figure W1*Cii*) where MDAMB231 tumor tissue again stained weakly positive (Figure W1*Ci*). Importantly, the background signal found on formalin-fixed tumor tissue slices was relatively low (Figure W1, *B* and *C*).

Discussion

CXCR4-overexpressing cell lines rather than CXCR4-transfected cell lines. The CXCR4-negative and -positive cell lines used have a small (factor = 2.4-7.5) difference in CXCR4 expression levels (Table 1). Clearly, this minor difference makes it more difficult to differentiate between the two expression levels using FIHC. This is especially so because the MDAMB231 cell line cannot be considered completely CXCR4-negative but has a basal CXCR4 expression. CXCR4-transfected and/or downregulated cell lines would make the differences much clearer. However, we reasoned that differences in clinical breast tumor samples would also be marginal because an up-regulation factor of 5.5 has been reported [3].

Because of this similarity in overexpression, we consider the difference between our MDAMB231 cell lines more representative for the clinical situation, and thus, this experimental setup may better predict the potential clinical value of the approach.

Intravenous administration of Ac-TZ14011–FITC. To overcome the fixation artifacts seen in fixed cells and tumor tissue and to study CXCR4 expression of the tumor tissue in its most natural environment, Ac-TZ14011–FITC was intravenously administrated to tumor-bearing mice (Figure W1*A*). Analysis of the freshly isolated tissue before or after fixation revealed stronger staining of the cytoplasm of MDAMB231^{CXCR4+} tumor tissue compared with MDAMB231 tumor tissue (Figure W1, *B* and *C*). Because it can be expected that the membranous staining in these tumor cells is internalized after the incubation period, these results are in line with those obtained for viable tumor cells at RT (Figure 1*C*).

Table W1. SDF-1 Prevents Binding of 12G5-PE and Ac-TZ14011–FITC to the CXCR4 Receptor (n = 3).

	Cell Type	
	MDAMB231^{CXCR4+}	
	MFIR ± SD	%
12G5-PE	1.485 ± 0.018	
SDF-1 + 12G5-PE	1.274 ± 0.033	−14*
Ac-TZ14011–FITC	5.184 ± 0.144	
SDF-1 + Ac-TZ14011–FITC	3.699 ± 0.034	−29*

For significance: 12G5-PE/Ac-TZ14011–FITC MFIRs were compared to MFIRs of SDF-1 + 12G5-PE/Ac-TZ14011–FITC incubated conditions.
% indicates percentage change in fluorescent signal intensity.
*$P \leq .005$.

References

[1] Nomura W, Tanabe Y, Tsutsumi H, Tanaka T, Ohba K, Yamamoto N, and Tamamura H (2008). Fluorophore labeling enables imaging and evaluation of specific CXCR4-ligand interaction at the cell membrane for fluorescence-bases screening. *Bioconjug Chem* **19**(9), 1917–1920.

[2] Zhang Y, Foudi A, Geay JF, Berthebaud M, Buet D, Jarrier P, Jalil A, Vainchenker W, and Louache F (2004). Intracellular localization and constitutive endocytosis of CXCR4 in human CD34^{+} hematopoietic progenitor cells. *Stem Cells* **22**(6), 1015–1029.

[3] Kang H, Watkins G, Douglas-Jones A, Mansel RE, and Jiang WG (2005). The elevated level of CXCR4 is correlated with nodal metastasis of human breast cancer. *Breast* **14**, 360–367.

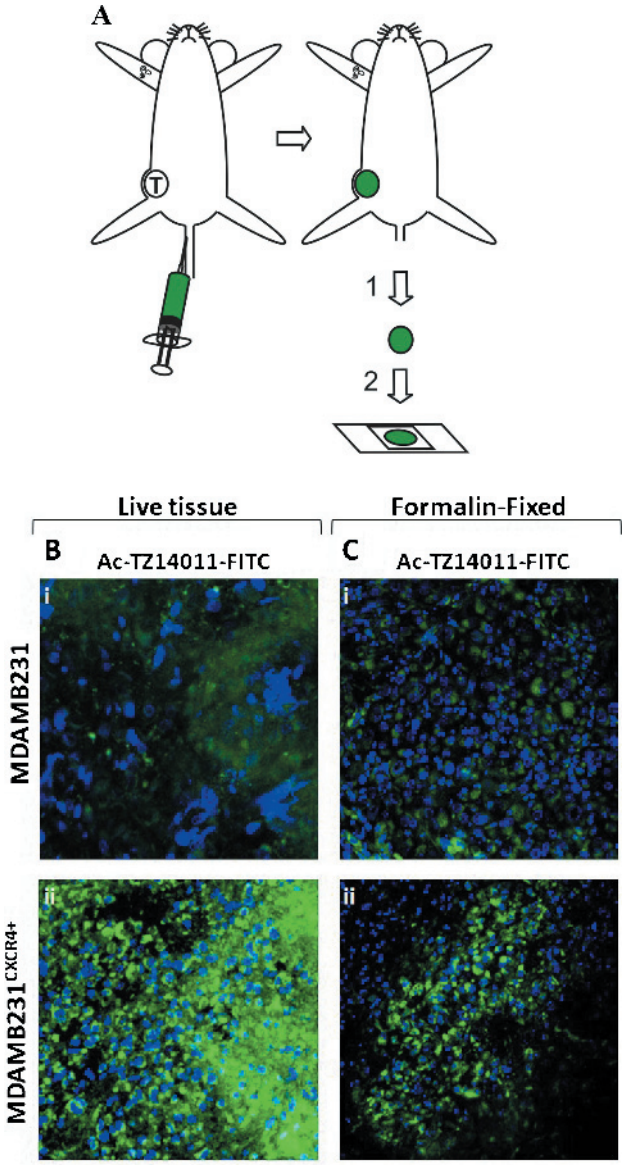

Figure W1. Predominantly cytoplasmic CXCR4 expression in *in vivo* Ac-TZ12011–FITC–incubated MDAMB231^{CXCR4+} tumor tissue. (A) Schematic overview of the principle of intravenously Ac-TZ14011–FITC incubation: 1. Mice were killed, and the tumor was isolated 24 hours after 50 μg of Ac-TZ14011–FITC was intravenously injected; 2. Tumors were cut into thin slices and placed on a coverslip; 3. Confocal images were taken. (B) Confocal images of live tumor tissue. Original magnification, ×630. Controls were less positive (data not shown). (C) Freshly isolated tumor tissue was formalin-fixed and imaged. Original magnification, ×400. Controls were negative (data not shown).